Soft Fingertip in Probing *

Yefan Zhou[1] Junyan Su[2] Jieming Li[3]

***Abstract*— In this project, we build a depth camera-Based soft fingertip device which is attached to a robotic arm. Three experiments are designed to explore the property and application of our device. First, a force reconstruction experiment is setup to find the relation between the force and the shape of our device. Second, the possibility of stiffness estimation is explored. Third, a software to perform 3D-probing is developed. Results show the outstanding performance of the device. Some future improvement is then discussed. Our website is linked here.**

I. INTRODUCTION

With the emerging robotics technologies, robots are becoming an indispensable part of our society. However, due to their rigid body nature, traditional robots have limitations in performing tasks such as sensing objects or environments while they are interacting. Most of the traditional robots rely on external cameras or LIDAR to capture the characteristics of environments for them. However, this way of sensing is far from perfect since the space in complex environments can be unreachable to robots as light travel in straight lines. Soft robots, however, are able to go into the narrow gap with some complex structures which makes it possible to get physical information of the environments just like we do using our hands. The recent progress in this area has been applied to challenging tasks, including legged locomotion [1] and dexterous grasping [2]. However, there remains a lot research space in a new proposed device blueprint, pneumatically-driven systems [3]. The potential capability of this soft system has been revealed in previous work [4], but the further exploration and relevant application is desirable in robotic tasks. In this work, we utilize a similar design of pressurized tactile sensor equipped with off-the-shelf depth-sensing camera [5]. First we develop the sensing capability for simple convex object and flat plane. We then develop an empirical model relating force, deformation and initial air pressure. Based on the force model, we propose a method that uses robot arm to manipulate this device and execute stiffness estimation. We further explore the utility of shape sensing and stiffness estimation in practical application, probing a uninformed environment and get visualization of contact shape and stiffness information.

* This work is a course project of EE106B at UC Berkeley, 2019. As a complement, a website is designed for the vedios and further information of this project: https://softfingertip.weebly.com

[1] Yefan Zhou is a Junior exchange student at UC Berkeley yefan0726@berkeley.edu

[2] Junyan Su is a Senior exchange student at UC Berkeley sujy@berkeley.edu

[2] Jieming Li is a Senior mechanical engineering student at UC Berkeley jiemingli@berkeley.edu

II. RELATED WORK

The design of soft tactile sensing device remains an active area of research. The objective of tactile sensing is measuring information about contact area during physic interaction [6]. To accomplish that, novel designs with embedding of rigid materials such as fiber [7] or electronic sensor [8] are proposed to conduct sensing data. However, this design imposes constraints on maximum material strain and limit the deformation of soft material. This challenge has been overcome by image-based methods. Yamaguchi et. al. [9] developed a soft tactile sensor FingerVision that uses a transparent skin with markers tracking by single RGB camera, which is successfully applied in gripper to extract and reconstruct normal and sheer force in grasping. The paper[10] developed a tactile sensor with an elastomer gel membrane, which uses a coaxial camera and illumination by multiple LEDs to capture high-resolution height maps of object surfaces. Both the two methods are excellent and competent in sensing resolution and accuracy but their probing range are all small because they purely utilize the visual information like image and light reflection. [4] concentrates on the analysis of membrane deformation with larger shape and force sensing range but relatively lower resolution which is based on the research in [11]. The employment of depth camera in [5] mitigates the contradiction of resolution and range by analyzing the point cloud [12] to extract geometric information of membrane which is exactly the foundation of our work. We also explore the utility of this device in surface probing under the guidance of [13].

III. DEVICE DESIGN

For the hardware designs, we adopt most of them from Isabella Huang, who is a graduate student in Professor Bajcsy's lab and she is one of the authors who proposed the possibility of making soft robot fingertip to detect environments. After some adjustments, the system we use is shown as figure 1
The adjustments we make are mostly on the capsule and the connection between it and the Baxter robot arm. Based on the feedback from Isabella, we increase the diameter of the capsule so that we can achieve a more accurate estimation of the deformation of the soft fingertip surface. The designs and the process of making them are shown below:
However, making the capsule bigger also brings out other issues such as maintaining the position of the inserted camera and how to firmly attach it to the robot arm. Therefore, we redesign the capsule with two connecting parts and design a bridge to connect it and the arm. We then use Type-A 3D printer to print out the parts with 100 percent infill density and achieve good results.

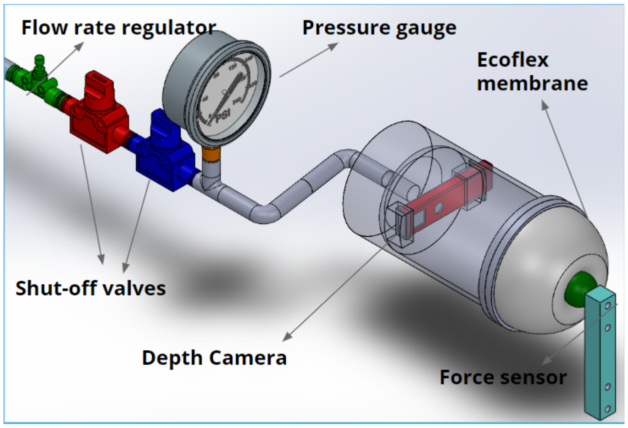

Fig. 1: Overview of the hardware system

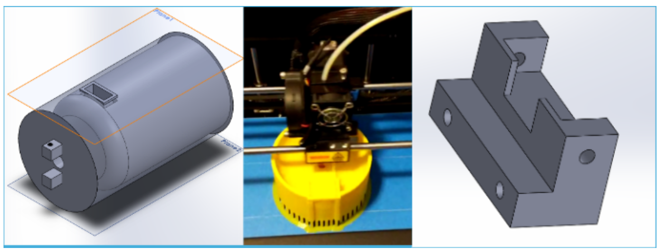

Fig. 2: CAD view of the major parts

IV. Method

A. Contact Region Reconstruction

The goal of contact region reconstruction is to estimate the geometry of the obstacle with point cloud stream from the camera. The expected performance is that we can accurately mark the deformed area and contact area in the raw point cloud of membrane. Since the imaged elastic membrane deforms to the shape of the obstacle it touches, we can infer the object shape by tracking the deformation of membrane. The region reconstruction is basically the segmentation of two classes:

- **Deformed**: Surface element undergoes a non-rigid transformation post-contact.
- **Contacted**: Surface element is both in contact with the obstacle and undergoes a non-rigid transformation post-contact.

For deformed area, we utilize spatial dynamic detection based on 3D data structure Octree [14]. We save the prior-deformed point cloud and compare each subsequent frame of point cloud with it, and mark the changing part as deformed area.

For contact area, we simply approximate our contact area as two classes: convex surface and plane surface. Since our membrane is absolutely pressurized, from the view of camera, the area contacting object is convex or flat and other un-contact part is concave. We thereby follow the computationally efficient method presented in [12]. The convexity test is accomplished by the local curvature signal, κ, estimated as:

$$\kappa\left(\mathbf{x}_i, \mathbf{y}_i\right)=\left\langle p_s\left(\mathbf{x}_i\right)-p_s\left(\mathbf{y}_i\right), p_n\left(\mathbf{x}_i\right)-p_n\left(\mathbf{y}_i\right)\right\rangle \quad (1)$$

where $\langle . \rangle$ is the dot product and $p_s(\mathbf{x})$ is the 3D spatial point. The criterion of classification is defined as:

- $\kappa > 0$: concave
- $\kappa = 0$: flat
- $\kappa < 0$: convex

We traverse through all the points in every frame of point cloud and select the four nearest neighbour points, calculating and judging the convexity signal in vertical and horizontal direction.

B. Force Reconstruction

The goal of the force reconstruction is to recover the membrane loads that transformed it from its initial body shape to a subsequent deformed one. The procedure is nonlinear and complex due to the property of elastic material. Therefore, we approximate our hemisphere elastic membrane at each internal gas state as an equivalent linear isotropic elastic sphere. In that case, Hertz contact relationship [15] between the load force F and the indentation depth δ can be applied to our force reconstruction as a reference model:

$$F=\frac{4}{3}\left(\frac{1-\nu_1^2}{E_1}+\frac{1-\nu_2^2}{E_2}\right)^{-1}\left(\frac{1}{R_1}+\frac{1}{R_2}\right)^{-1/2} \delta^{3/2} \quad (2)$$

where E_i, and R_i, and v_i are the elastic modulus, radius, and Poissons ratio of each equivalent elastic sphere.

C. Stiffness Estimation

To estimate the stiffness of a contact point, we keep track of the robotic arm's movement in z, denoted by D, and the largest deformed depth δ. Thus, the displacement of a contact point in the contact surface (not the fingertip) is $D-\delta$. Assume we have a function $F: \mathbb{R} \rightarrow \mathbb{R}$ which maps from δ to the contact force. To estimate the stiffness of a contact point, we simply use a linear model:

$$k=\frac{F(\delta)}{D-\delta} \quad (3)$$

Note that the assumption that the stiffness model is linear is probably not practical. We use this model, however, as a start to explore if we can use our hardware device to characterize the stiffness property of a certain object.

D. 3D probing

The goal of 3D probing is manipulating a robot arm mounted by a soft fingertip sensor to scan an uninformed area, and visualize the shape and height map of this area as well as the stiffness information demonstrated by different color. The inspiration comes from our own biological fingertips, in that objects of interest usually have to be probed from many different directions before we can infer their structures. Basically, we will initialize a point cloud object at first, and then in scanning procedure, constantly adding 3D spatial points that judged as the point in contact area of membrane. We make translation according to robot arm movement, make rotation according to the transform between camera frame and world frame. At the meantime, calculating the received force and the stiffness of contact area based on the method mentioned above and changing the color of point cloud in visualization according to the stiffness degree of contact object.

V. Results

A. Contact Region Reconstruction

As shown in Fig. 3, we use a rigid plastic sphere and the desk as contact object to test the shape sensing ability. Fig. 4 shows a good correspondence between the geometry of the estimated contact region with that of the real obstacle. However, validation shows that our method sometimes overestimate the actual contact area because our assumption that air pressure can perfectly distinguish contact and non-contact as concave and convex is not exactly right. There remains error of small non-contact area surrounding the object when interaction could show the feature of contact area from view of camera as air pressure are not able to prevent their deformation.

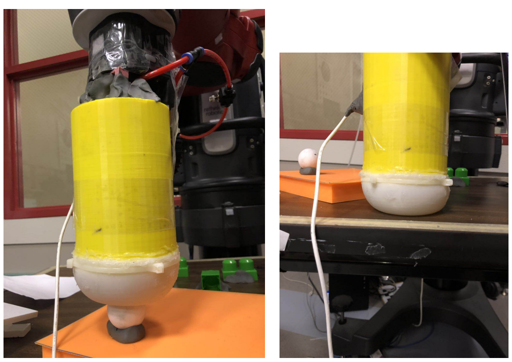

(a) a

(b) b

Fig. 3: (a) shows the contact with rigid plastic sphere. (b) shows the contact with flat plane.

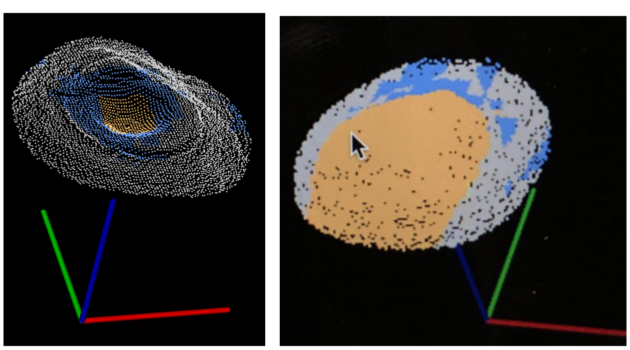

(a) a

(b) b

Fig. 4: (a) shows the segmented point cloud when sensor contacts a sphere. (b) shows the segmented point cloud when sensor contacts a flat plane. Blue area is deformed but non-contact area. Red area is deformed and contact area.

B. Force Reconstruction

For our hardware setup shown in Fig.5, we prepare two mold as contact object: rigid plastic sphere with diameter of 40mm and rigid square plane with edge length of 120mm. We collect six datasets with air pressure 1 psi [1], 1.5 psi, 2 psi for two shape of contact object. At each time step, the indentation depth δ was measured directly by the depth camera, and the axial force F_z by the load cell.

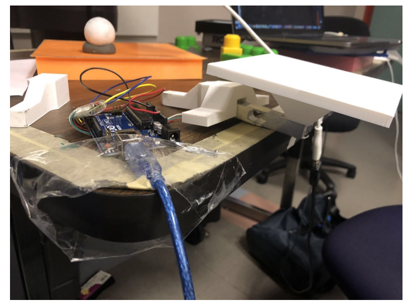

Fig. 5: Hardware setup for force reconstruction. Arduino, Load cell, 40mm diameter sphere object and plane object

These results are plotted in Fig. 6. Then, for each plotted curve given a fixed initial gas state characterized by air pressure, linear regression was performed and the fitted slopes were recorded. Left figure in Fig. 6, Hertz contact model fits our case when our sensor contact with a sphere, the polynomial order of indentation is close to $\frac{3}{2}$ in IV-B. However, for the plane contact, the relationship displays higher order than that in reference model and the Hertz contact model doesn't fit well. Even though we can still find an approximate polynomial curve to fit it. The curve can be used as an efficient empirical model as we need in real time force calculation. The inadequacy of Hertz model is in our expectation as in this case, we set the R_2 in IV-B to be infinite and this approximation has not been proved. Besides, our setup doesn't meet the requirement of Hertz contact model of contact between two uniformly solid elastic object. As a result, for spherical and planus geometries, a deterministic relationship between membrane deformation and its resulting force was realized.

Based on this model, we can implement force estimation and visulization in real time, changing the brightness of color in displaying point cloud according to the degree of force calculated. Note that this application in our project is not accurate enough as a force sensor due to its low resolution and empirical model, it mainly provides a good support for stiffness estimation as it only needs a rough estimation of force.

[1]The degree of air pressure: Pounds per square inch

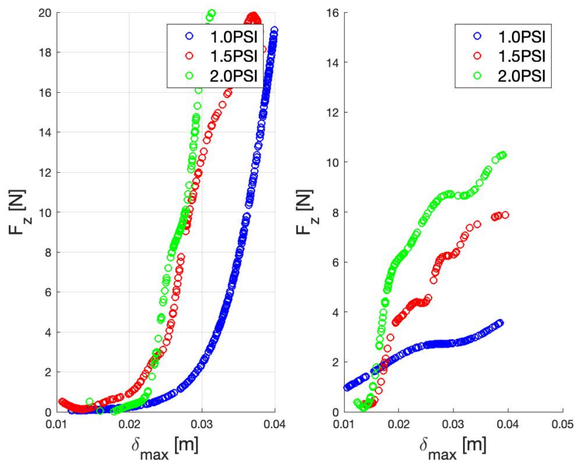

Fig. 6: Plots for relationship between force and indentation The left figure is the relationship about contact with plane. The right figure is the relationship about contact with sphere. x axis represents max indentation of membrane, y axis represents force. Blue line represents the air pressure of initial state is 1.0 psi, red line represents 1.5 psi, green line represents 2.0 psi.

C. Stiffness Estimation

As shown in Fig. 7, we build the testing materials with ecoflex10 and ecoflex50. The frame to hold the testing masterials is 3d-printed. Then a trajectory for robotic arm to move upside down is executed. Multiple data with different air pressure is then collected for further analysis. We collect six datasets with air pressure 1psi, 1.5psi, 2psi for each materials.

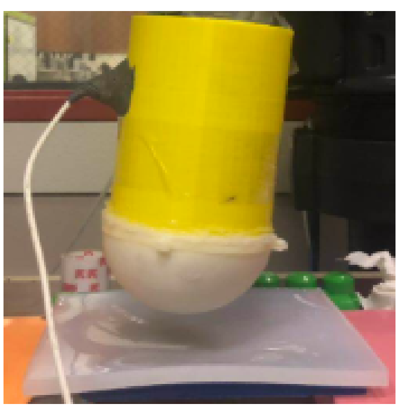

Fig. 7: Hardware setup for stiffness Estimation

Figure 8 are the plots of data we collect. As shown, the left part is the plots for ecoflex10, and the average slopes of the three lines is about 0.15 and the average slopes for ecoflex50 is about 0.20. If we assume the function F is a linear map from δ to the force f, then the estimated stiffnesses are 0.175 and 0.255 for ecoflex10 and ecoflex50, respectively. The results show that we can indeed characterize the stiffness of different materials. The signals we have are, however, very noisy and thus it is still unclear if we can estimate the stiffness online.

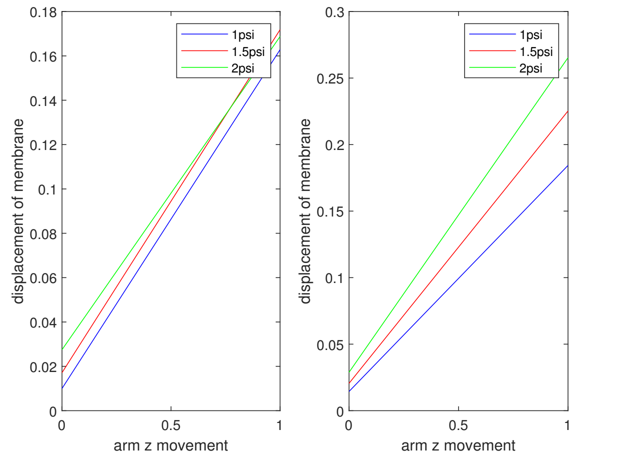

Fig. 8: Plots for stiffness estimation with different materials and air pressures.

D. 3D probing

We successfully implement the basic scheme of manipulation, perception and visulization by combing the result of three parts above. The difficulty in this part is making right transformation to join the individual point cloud fragment generated in per poking action to reconstruct the overall shape of object. We first set the visualization world frame as the hand frame as shown in Fig. 9 (a). We apply a reflection matrix and a rotation matrix to every frame of point cloud and then translate it according to the position of robot arm. The visualization performance is shown in Fig. 9 (b).

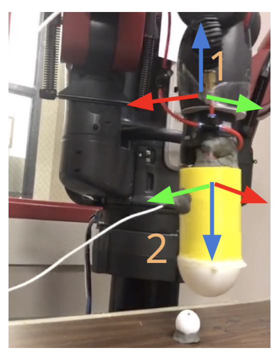

(a) a

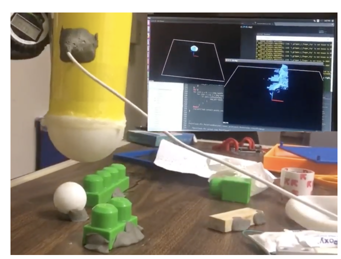

(b) b

Fig. 9: In (a), 1 is the world frame, 2 is the camera frame. In (b), the green building blocks are estimated object, the blue image in right upper corner is the visualization of their shape.

VI. Conclusions

In this report, some applications for a depth camera-Based soft fingertip device[5] is presented. In particular, force reconstruction, stiffness estimation and 3D-probing are implemented to explore the property of this device. Results show that our device is suitable for those applications. However, since the time is limited, there are several possible future extensions:

- *Force Reconstruction.* For force reconstruction, we use Arduino with force sensor to measure the correspond force associate with image outputs.
- *Stiffness Estimation.* For stiffness estimation, we simply use a linear model. This is not practical and a better model might be useful.
- *3D probing.* Due to the inaccuracy of the robotic arm, we are not able to perfectly reconstruct the shape of an object. In particular, the coordinate of two probings are not cohesive. A better robotic arm with high accuracy or a more sophisticated filter or algorithm can be applied for better performance.

REFERENCES

[1] M. T. Tolley, R. F. Shepherd, B. Mosadegh, K. C. Galloway, M. Wehner, M. Karpelson, R.J. Wood, and G. M. Whitesides. A resilient, untethered soft robot. *Soft Robotics*, 1:213–223, 11/27/2013 2014. 1224.

[2] F. Ilievski, A. D. Mazzeo, R. F. Shepherd, X. Chen, and G. M. Whitesides. Soft robotics for chemists. *Angew. Chem.*, 50:1890–1895, 10/5/10 2011. 1112.

[3] A. Stilli, L. Grattarola, H. Feldmann, H. A. Wurdemann, and K. Althoefer. Variable stiffness link (vsl): Toward inherently safe robotic manipulators. In *2017 IEEE International Conference on Robotics and Automation (ICRA)*, pages 4971–4976, May 2017.

[4] D. Hristu, N. Ferrier, and R. W. Brockett. The performance of a deformable-membrane tactile sensor: basic results on geometrically-defined tasks. In *Proceedings 2000 ICRA. Millennium Conference. IEEE International Conference on Robotics and Automation. Symposia Proceedings (Cat. No.00CH37065)*, volume 1, pages 508–513 vol.1, April 2000.

[5] I. Huang, J. Liu, and R. Bajcsy. A depth camera-based soft fingertip device for contact region estimation and perception-action coupling. In *2019 IEEE International Conference on Robotics and Automation (ICRA)*, May 2019.

[6] R. S. Dahiya, G. Metta, M. Valle, and G. Sandini. Tactile sensingfrom humans to humanoids. *IEEE Transactions on Robotics*, 26(1):1–20, Feb 2010.

[7] C. Larson, B. Peele, S. Li, S. Robinson, M. Totaro, L. Beccai, B. Mazzolai, and R. Shepherd. Highly stretchable electroluminescent skin for optical signaling and tactile sensing. *Science*, 351(6277):1071–1074, 2016.

[8] Nanshu Lu and Dae-Hyeong Kim. Flexible and stretchable electronics paving the way for soft robotics. *Soft Robotics*, 1(1):53–62, mar 2014.

[9] A. Yamaguchi and C. G. Atkeson. Implementing tactile behaviors using fingervision. In *2017 IEEE-RAS 17th International Conference on Humanoid Robotics (Humanoids)*, pages 241–248, Nov 2017.

[10] R. Li, R. Platt, W. Yuan, A. ten Pas, N. Roscup, M. A. Srinivasan, and E. Adelson. Localization and manipulation of small parts using gelsight tactile sensing. In *2014 IEEE/RSJ International Conference on Intelligent Robots and Systems*, pages 3988–3993, Sep. 2014.

[11] Nicola J. Ferrier and Roger W. Brockett. Reconstructing the shape of a deformable membrane from image data. *The International Journal of Robotics Research*, 19(9):795–816, 2000.

[12] E. R. Nascimento, G. L. Oliveira, M. F. M. Campos, A. W. Vieira, and W. R. Schwartz. Brand: A robust appearance and depth descriptor for rgb-d images. In *2012 IEEE/RSJ International Conference on Intelligent Robots and Systems*, pages 1720–1726, Oct 2012.

[13] Pramath Raj Sinha and Ruzena Bajcsy. Active exploration of surfaces for legged locomotion of robots. 1990.

[14] Tsz Ho Wong, Geoff Leach, and Fabio Zambetta. An adaptive octree grid for gpu-based collision detection of deformable objects. *The Visual Computer*, 30(6):729–738, Jun 2014.

[15] Susendar Muthukumar and Reginald DesRoches. A hertz contact model with non-linear damping for pounding simulation. *Earthquake engineering & structural dynamics*, 35(7):811–828, 2006.